J Appl Electrochem (2012) 42:615–626
DOI 10.1007/s10800-012-0438-9

ORIGINAL PAPER

The influence of electrolyte composition on electrochemical ferrate(VI) synthesis. Part III: anodic dissolution kinetics of a white cast iron anode rich in iron carbide

Zuzana Mácová · Karel Bouzek

Received: 6 March 2012 / Accepted: 5 June 2012 / Published online: 20 June 2012

Abstract The anolyte composition and process temperature could improve the kinetics of iron anode dissolution and subsequent ferrate(VI) production significantly. This also holds for the anode composition. Following pure iron and silicon-rich steel (SRS), white cast iron (WCI) was the last representative of anode material tested that is typically used to produce ferrate(VI). Using anolytes 14 M NaOH, 14 M KOH, and mixtures thereof, the systems were studied by potentiodynamic methods, electrochemical impedance spectroscopy, and batch electrolysis experiments. Additionally, metallographic analysis of the material was performed. The dissolution kinetics increases with increasing temperature and also, at 60 °C, with increasing K^+ content in the anolyte, but less progressively than in the case of SRS. Similar to SRS, WCI also easily dissolves into ferrate(VI) even at 20 °C in pure NaOH, thus indicating the inferior protective properties of oxo-hydroxide surface layers. In general, a maximum current efficiency of approx. 60 % was obtained at 60 °C in pure KOH solution. The authors conclude that, at 60 °C, the high efficiency of the synthesis is caused by the low protective properties of the oxo-hydroxide surface layer caused by the preferential dissolution of cementite and at the same time by the precipitation of the potassium salt of the product in the electrolyte immediately after its formation. This minimizes the effect of its decomposition.

Z. Mácová · K. Bouzek (✉)
Department of Inorganic Technology, Institute of Chemical Technology Prague, Technická 5, 166 28 Prague 6, Czech Republic
e-mail: bouzekk@vscht.cz

Keywords Ferrate(VI) · Dissolution kinetics · Iron carbide · Electrolyte composition · Electrode composition

1 Introduction

This paper represents the final part of a series of studies dealing with the influence of the electrolyte composition, namely the content of Na^+ and K^+ ions at constant OH^- concentration, on the process of anodic dissolution of three basic iron alloys typically used for ferrate production [ferrate means ferrate(VI) throughout this text]. The first part of the series [1] focused on pure iron as an anode material, the second part [2] on silicon-rich steel (SRS) as an electrode. As discussed in these papers, the selection of materials was mainly motivated by our previous studies [3, 4]. Pure iron is used as a reference point to reduce the number of variables in the system regarding the anode structure and composition, and thus to assess the influence of the individual additional components on electrode behavior [3]. On the other hand, SRS was considered in order to evaluate the influence of the presence of Si in the material structure on the ferrate synthesis process [4]. In agreement with [5, 6], the important influence of anolyte composition on the properties of the system and, as a consequence, on ferrate synthesis efficiency was observed for both the materials. The aim of this paper is to complete this study by evaluating the influence of the presence of iron carbide (Fe_3C) in the material structure on the ferrate synthesis process. White cast iron (WCI), being a material rich in this component, was used for the declared purpose [7].

WCI has been intensively studied in the past in the context of ferrate synthesis on account of its superior properties with respect to the efficiency of this process at

higher current densities. Such behavior was explained in terms of the presence of Fe_3C in the structure of this material [7]. This component of the structure of WCI was observed to dissolve more progressively in a strongly alkaline environment under anodic polarization than the remaining ones. By this means it caused a continuous renewal of the fresh electrode surface in contact with the anolyte which in turn resulted in the gradual passivation of the anode surface to be suppressed [7]. A more detailed and complex discussion of the influence of the material and the electrolyte composition is provided in a review of electrochemical ferrate synthesis [8].

To date, there is a lack of detailed information on the influence of anolyte composition on ferrate synthesis by this particular material in the literature. Such information is of great interest since WCI has shown highly promising properties for this process when used in concentrated NaOH solution as an anolyte. Moreover, it completes the series of in-depth studies on the two above-mentioned types of materials [1, 2]. It thus allows a more profound understanding of the combined influence of the anode material and anolyte composition on the ferrate synthesis process.

As in the previous studies, potentiodynamic voltammetric (PV) experiments, electrochemical impedance spectroscopy (EIS) measurements and batch electrolyses were used to identify the dissolution mechanism of WCI. The investigations were conducted in electrolytes similar to those specified in [1, 2] and similar experimental conditions were applied. This made it possible to compare the characteristics obtained using WCI with those of SRS and pure iron. Furthermore, SEM images and metallographic analysis were used in order to detect changes in the surface state.

2 Experimental

A detailed description of the chemicals, apparatus, and procedures used can be found in [1]. The following information is supplementary. The PV and EIS experiments were performed in a classical three-electrode arrangement. The working electrode had an active surface of 0.283 cm^2 and contained 3.17 wt% C in the form of Fe_3C and the following impurities: 0.44 wt% Mn and 0.036 wt% Ni. The inactive electrode surface was insulated by Teflon (RRDE). The ring electrode for the experiments on a rotating ring-disk electrode was made of platinum. Its potential was held at a value corresponding to the FeO_4^{2-} reduction, i.e., at 300 mV [9, 10]. The results are related to an HgO/Hg reference electrode with 14 M NaOH as the internal electrolyte. The counter-electrode was a platinum foil with an active surface of 0.84 cm^2. The working electrode was cathodically pre-polarized at 20 mA cm^{-2} for 5 min before each experiment. In the case of the PV experiments, a recording of the polarization curve at the studied sweep rate (5–500 mV s^{-1}) immediately followed pre-polarization. In the case of the EIS experiments, the electrode potential was held at a required value for 10 min and then an impedance spectrum was recorded in the frequency range of 60 kHz–10 mHz. An *ac* signal amplitude of 10 mV was used. All experiments were performed under nitrogen atmosphere.

The batch electrolyses were carried out in galvanostatic mode in a cell with a PVC diaphragm separating the anode and cathode compartments. The active surface of the anode was 66.8 cm^2 and the anolyte volume was 95 cm^3. The galvanostatic experiment was carried out for 180 min after 30 min cathodic pre-polarization at 20 mA cm^{-2}.

Before metallographic analysis, the sample of anode material was polished with P4000 emery paper (Buehler, USA). The sample was then etched in a 2 % HNO_3 solution in ethanol for approximately 2 min at room temperature.

Before SEM analysis, the following procedure was applied: the polished electrode surface was cathodically pre-polarized at a current density of 20 mA cm^{-2} for 5 min. The polarization was then immediately switched to anodic and a current density of 15 mA cm^{-2} was applied for 15 min. After polarization, the electrode was rinsed with distilled water, dried in hot air, and analyzed immediately. During electrode preparation, 14 M KOH or 14 M NaOH was used as the electrolyte at temperatures of 20 or 60 °C.

3 Results and discussion

3.1 Voltammetric experiments

The cyclic voltammetric (CV) curves of the WCI electrode in 14 M NaOH and KOH at 20 and 60 °C are shown in Fig. 1. With this electrode, the recorded voltammograms also show characteristics similar to the previous two materials. Therefore, the individual current peaks observed on the polarization curves in the two electrolyte solutions at 20 °C (Fig. 1) can be ascribed to reactions similar to those for an iron [1] and an SRS [2] electrode:

Peak AI	Oxidation of metallic Fe–Fe(II)	Eq. (1) in [1]
Peak AII	Oxidation of Fe(II)–Fe(III)	Eq. (2A–C) in [1]
Peak AIII	The restructuring of the anode surface layer	
Peak AIV	Reactions related to ferrate formation	Eq. (6) in [1]
Peak CIII	Ferrate reduction to Fe(III)	
Peak CII	Reduction of the surface layer from Fe(III) back to Fe(II)	
Peak CI	Subsequent Fe(II) reduction to Fe(0)	

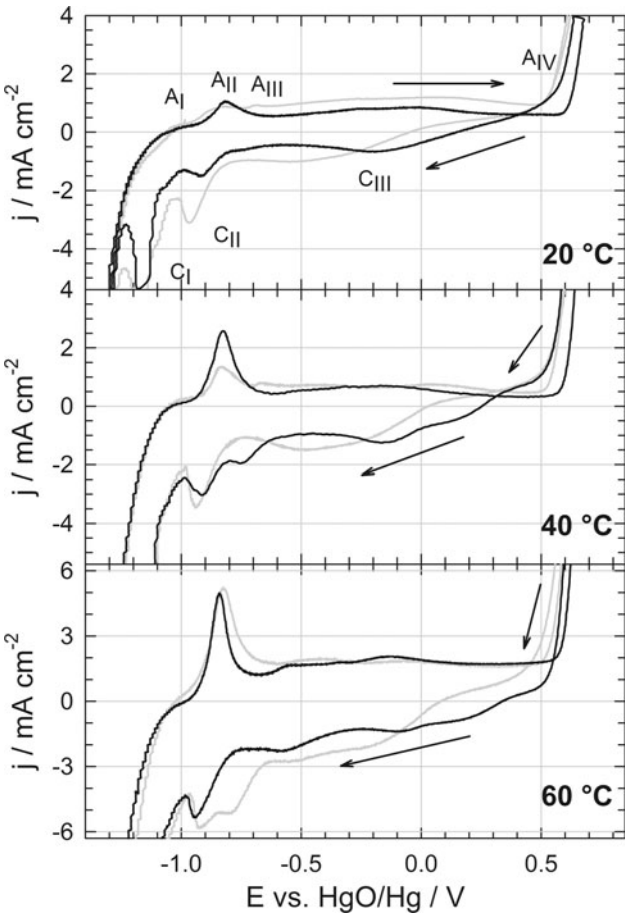

Fig. 1 The polarization curves of the WCI electrode in NaOH (*black*) and KOH (*gray*) at a sweep rate of 5 mV s^{-1}. The temperature is indicated on the graphs; *arrows* indicate the potential sweep direction

Compared to pure iron and SRS, in the present work, WCI shows a significantly less pronounced peak AI in NaOH at 20 °C. Additionally, peak AIII was not observed in NaOH at 20 °C. This indicates the absence of the corresponding restructuralization of the surface layer under the given conditions. This may be attributed to the electrode structure of WCI, leading to a disrupted oxo-hydroxide surface layer. In the case of KOH, the current peaks are generally better defined and even peak AIII is again visible on the voltammogram. This corresponds to the reduced solubility of the electrode dissolution products in this electrolyte, resulting in a better developed surface film.

On the other hand, using KOH electrolyte, a higher current density was obtained in the potential region of electrode passivity than in the NaOH solution. This is connected with more intensive interaction of the oxo-hydroxide layer covering the electrode surface with this electrolyte. The anodic current peak AII is a further interesting aspect. It dominates over the other peaks and the difference rapidly increases with temperature. Thus, it is clearly connected with the presence of the Fe_3C phase in the anode structure. At 60 °C the dominating current peak AII becomes equally intensive for both the electrolytes used. During the anodic potential scan, the behavior of the electrode is similar in both the electrolytes. Only in the case of NaOH solution can current peak AIII be distinguished better on the voltammogram. Under these conditions, an additional peak AIIIB also appears in the potential region of −0.13 V on the voltammogram. This is a similar situation to SRS, where a comparable peak, increasing with increasing temperature, was observed [2]. However, with SRS, this peak appeared in KOH solution and was significantly more pronounced than in the case of WCI.

With regard to the cathodic scan of the electrode potential, the situation is more interesting. Here, the WCI electrode shows a characteristic very close to that of SRS. With increasing temperature, current peak CII separates into two peaks, CIIA and B, the separation being more visible in the case of KOH as an anolyte. Such behavior indicates that it is connected with the presence of the related oxidized reactant on the electrode surface in the solid form. Moreover, the shift of the peak CIII potential to more cathodic values in KOH, as compared to NaOH, corresponds to this phenomenon.

Similar to SRS, a significant hysteresis in the course of the polarization curve in the transpassive potential region was observed. Here, too, the reason is the substantial diminution of the inhibition of the electrode surface toward dissolution at strongly transpassive potentials. To a certain degree this is probably connected not only with the oxidative dissolution of the electrode, but also with intensive oxygen evolution, causing mechanical damage to the surface film.

The origin of the individual current peaks on the CV curve was also verified by means of RRDE with a Pt ring electrode. The Pt ring current responses obtained were identical to those reported previously for pure iron (Fig. 2 in [1]), hence they are not shown here. The only difference exists in the higher current response observed for the disk electrode in a potential region higher than 0.40 V, corresponding to the produced ferrate reduction (20 °C, 14 M NaOH, increase from 6 μA observed for pure iron to 18 μA observed for WCI; 60 °C, 14 M NaOH, increase from 350 to 650 μA).

The addition of K^+ ion to the basic NaOH electrolyte resulted in a shift of the start of the passivity potential region as well as of the current peak CIII potential to less anodic values. Similar to SRS [2], this indicates more pronounced passivation of the electrode surface. Tafel slope analysis in the potential region of current peak AIV also revealed (90–120 mV dec^{-1} for the temperature range 20–60 °C in all electrolytes) that, in the case of WCI electrode, too, this current peak corresponds to the process connected with the transfer of one electron. This is in

agreement with two materials studied previously [1, 2]. Here, too, the mechanism of ferrate formation can thus be considered uninfluenced by the change in the material and the structure of the electrode.

Furthermore, the dependence of current peaks AIV and CIII peak current on the potential sweep rate studied in the next step showed characteristics qualitatively similar to those of the SRS electrode. As shown in Fig. 2, the current density of peak AIV initially increases with the potential sweep rate. However, after reaching a maximum at a sweep rate of 100 mV s^{-1}, it starts to decline again. As with the previous materials, such behavior indicates that the mechanism of the reaction corresponding to this current peak is not purely electrochemical. It includes at least one chemical step becoming rate-determining at a potential sweep rate higher than 100 mV s^{-1}. In contrast to SRS, it is interesting to note that, with increasing temperature, the increase in the current density of peak AIV is significantly less pronounced. Whereas at 20 °C, the current density of peak AIV is more or less identical for SRS and WCI, at 60 °C, the value obtained for WCI reaches approximately 20–50 % of the value for SRS under identical conditions. For both the materials, the highest peak current density was attained with a K^+:Na^+ content of 1:1. In the case of WCI, the lowest peak current density was obtained for the electrolyte with a K^+:Na^+ content of 1:3. In the case of SRS, the increasing content of K^+ ion causes a current density decrease to a minimum.

The situation of peak CIII is only similar to that of SRS at 20 °C, where the peak current density increases in the entire potential scan rate under study. At 40 °C, it becomes stagnant at a potential sweep rate higher than 200 mV s^{-1}. At the highest temperature studied, i.e., 60 °C, the increase in current density stops at a potential sweep rate of 50 mV s^{-1}. Regarding the influence of the electrolyte composition, it is interesting that, while at 20 °C, the lowest peak current density was observed for the electrolyte containing K^+:Na^+ ions in a ratio of 3:1, at 60 °C, this solution provides the highest peak current density. The behavior of the pure KOH solution is exactly the contrary. The remaining electrolytes provide peak current densities within these limits.

From the point of view of the characterization of the electrode reaction, the kinetics of electric charge transfer provides extremely important information. Koutecky–Levich analysis was used to determine this parameter. A detailed description of the application of this method for our purposes is given in [1]. The plots obtained are shown in Fig. 3, where the general character of this dependence is similar to that of the previous materials (Fig. 3 in [1], [2]). The limited dependence on the electrode rotation rate indicates that the reaction is not influenced by the mass transport from the bulk of the electrolyte. On the contrary,

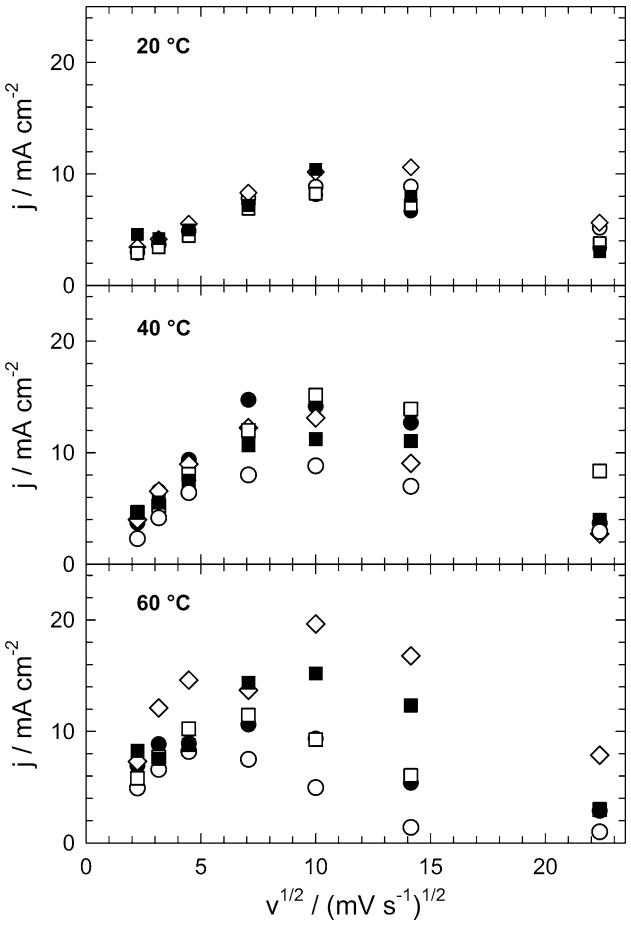

Fig. 2 The dependence of current density in the potential region of peak AIV on the square root of the potential sweep rate. Electrolyte composition: *filled circle* NaOH, *empty circle* Na^+:K^+ = 3:1, *diamond* Na^+:K^+ = 1:1, *empty square* Na^+:K^+ = 1:3, *filled square* KOH; the temperature is indicated on the graphs

at 20 °C the slope of the dependence is negative. Such behavior indicates that the reaction mechanism is disturbed by enhanced mass transfer between the bulk of the electrolyte and the electrode surface. One explanation is the removal of the ferrate formation intermediates from the electrode surface which becomes more intensive with enhanced electrode rotation rate, thus slowing down the overall reaction kinetics. At a higher temperature, the kinetics of the electrode reactions is enhanced. This is documented by the fact that the current density of peak AIV increases with increasing temperature independent of the electrode rotation rate. Ferrate formation is thus completed before the intermediates have been removed from the electrode surface. In this case, the influence of the electrolyte composition is not very pronounced. At 20 °C, mixed electrolytes show a slightly lower current density than pure electrolyte solutions. At 40 and 60 °C, the lowest current density was observed for the electrolyte containing K^+:Na^+ in a ratio of 1:3. However, the difference to the

other mixed solutions is fairly insignificant. Detailed results of the kinetic current density are shown in Table 1. From this table, at two lower temperatures the highest electrode reaction kinetics was observed for the pure NaOH solution. The remaining electrolyte compositions did not show any clear influence of the kinetic current density on this material. At 60 °C, the highest value of kinetic current density was obtained for pure KOH solution, its value being very close to the solution containing K^+:Na^+ ions in a ratio of 3:1.

Similar to SRS, in the case of WCI, an increasing electrode rotation rate did not have any significant impact on the shape of the CV curve. The only difference is the increase in current density in the potential region of electrode passivity during the anodic course of the electrode potential. During the cathodic potential course, the intensity of the current peaks declined. Both these phenomena may be explained in terms of enhanced convective mass transfer between the electrode surface and the bulk of the electrolyte solution. While in the case of the anodic potential course it results in enhanced chemical attack by OH^- ions on the oxo-hydroxide layer covering the electrode surface [11], during the cathodic potential sweep the removal of ferrate and intermediates from the anode surface reduces the extent of the electrode reactions corresponding to the individual current peaks.

3.2 EIS experiments

An example of the impedance spectra obtained for the WCI electrode is given in Fig. 4. Similar to the iron [1, 12] and SRS [2] electrodes, the process also exhibits two kinetic constants at the WCI electrode. Therefore, the physical model of two macrohomogeneous surface layers [1] was applied in this case, too. The theory of a duplex sandwich assembly of passivating layers was taken into account similar to [13], where the "passive pit" model [14] was used for data processing. An equivalent circuit expressing this model consists of two parallel R-CPE elements and one resistance element connected in series (see Fig. 5 in [1] for a detailed description). This approach minimizes the number of optimization parameters, while maintaining close agreement with physical reality. The solid lines in Fig. 4 represent the data calculated on the basis of an equivalent circuit using the parameters optimized from the experimental data. They confirm good agreement of the proposed model with the experimental data.

Figure 5 shows an example of the optimized equivalent circuit parameters for pure NaOH solution at the temperatures under study. The general shape of these dependencies is similar to that of the previous two materials [1, 2]. In the case of the outer oxidic layer, the decrease in the resistance value starts at a potential of 525–550 mV. This is associated with

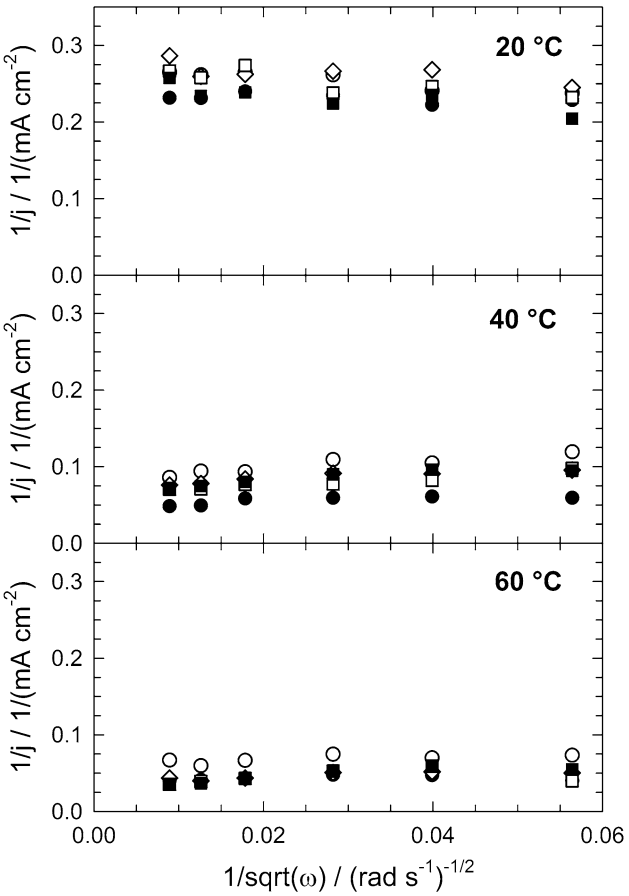

Fig. 3 The dependence of the reciprocal value of the current density in the potential region of peak AIV on the square root of the electrode rotational speed; for all rotation rates, current density was read at the same value of the electrode potential. Electrode: WCI; electrolyte composition: *filled circle* NaOH, *empty circle* Na^+:K^+ = 3:1, *diamond* Na^+:K^+ = 1:1, *empty square* Na^+:K^+ = 1:3, *filled square* KOH; the temperature is indicated on the graphs

the disintegration of this layer due to the commencement of the oxygen evolution reaction. In the case of the internal oxidic layer, the decrease already starts at a potential of 500 mV and is related to the initiation of anodic iron dissolution. On the other hand, the value of the capacity of the internal layer increases with increasing electrode potential up to its value of 550 mV. Afterward it remains more or less constant. The capacity of the external layer reaches a maximum at the same potential and, after exceeding it, starts to decline. In connection with the development of parameter ϕ, such behavior may be interpreted as being connected with the gradual reduction in thickness of the internal oxidic layer, permitting the steadily increasing dissolution of the base iron material. The situation of the external layer is less straightforward. The initial decrease in the ϕ value confirms mechanical damage to the layer by the evolved oxygen. Stabilization, or even a repeated increase, of the value of this parameter above a potential of 550 mV indicates stabilization of the external layer. The continuous decrease in its

Table 1 Values of the kinetic current density (mA cm^{-2}) of the WCI electrode in the potential region of peak AIV at the temperatures studied in 14 M OH^- solutions with various Na^+:K^+ ratios

Solution	NaOH	Na^+:K^+ = 3:1	Na^+:K^+ = 1:1	Na^+:K^+ = 1:3	KOH
j_K (°C)					
20	4.2 ± 0.1	3.7 ± 0.2	3.5 ± 0.2	3.8 ± 0.2	3.9 ± 0.3
40	21 ± 2	12 ± 1	14 ± 1	15 ± 1	14 ± 1
60	26 ± 2	17 ± 1	26 ± 2	34 ± 4	36 ± 5

resistance, however, must account for its practical disappearance. The resistance values involved are in the order of 1.0–0.1 Ω. It can be considered that significant parts of the external film are missing and that the decrease in the resistance value is connected with the gradual disappearance of a minor portion of the remaining film due to chemical and electrochemical interaction with the environment.

The dependence of the fitted parameters on the electrolyte composition is documented by data summarized in Fig. 6. This shows that, with regard to the resistance of the surface film, the trend observed for the two sublayers is a decrease in its value with increasing K^+ content. The significance of this decrease, in turn, decreases with increasing temperature, which is a result of the increasing kinetics of the chemical processes between the surface oxo-hydroxide layers and the electrolyte with increasing temperature. The capacitance of the surface films was influenced by the electrolyte composition in a slightly different way. Whereas at 20 °C the capacitance of the external layer decreased with increasing K^+ content, for the internal layer this characteristic remained constant. At 60 °C, by contrast, the capacity of the internal layer decreased significantly with K^+ content, whereas that of the external layer remained unchanged. Capacitance decreasing with K^+ content is related to the increasing thickness of the surface films. This phenomenon is caused by the decreasing solubility of the electrode dissolution products in the electrolyte incurred by increasing K^+ content. This is well visible only in the two above-mentioned cases and is characterized by a

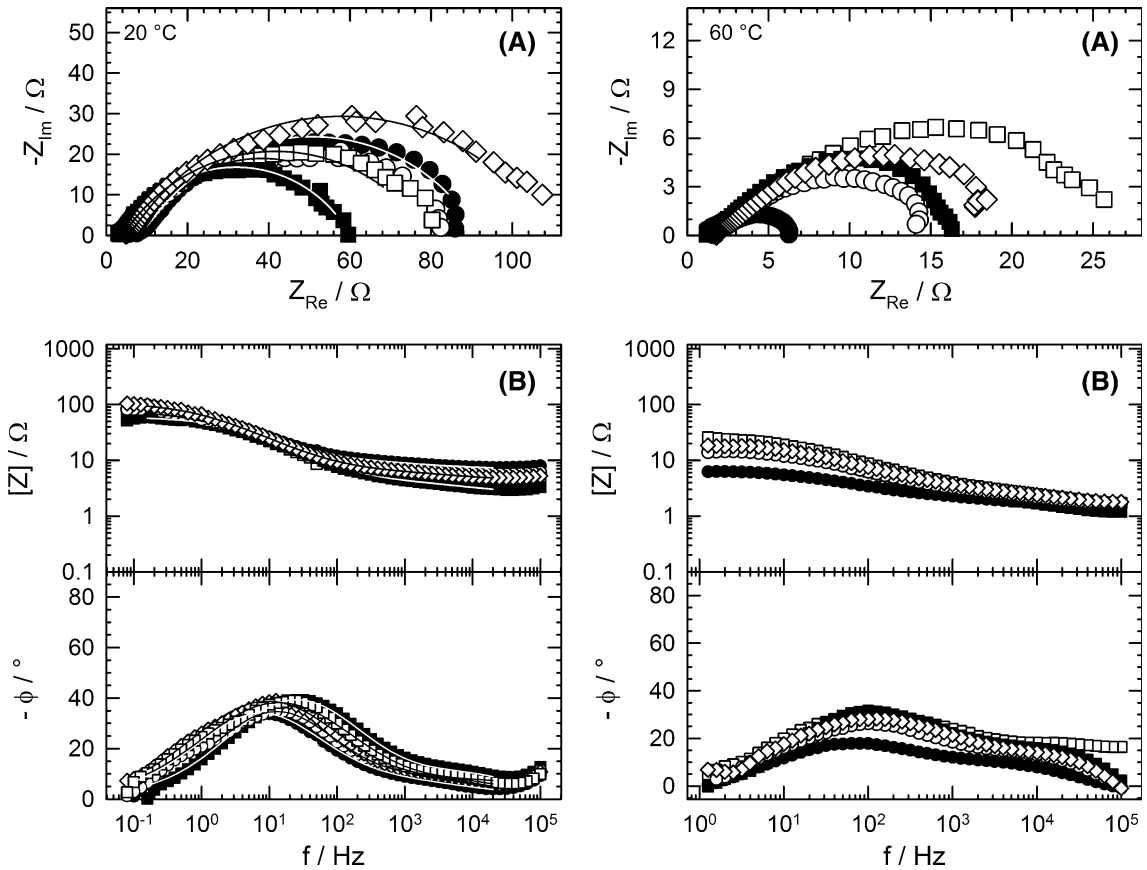

Fig. 4 EIS spectra of WCI in the electrolytes studied at 20 °C (*on the right*) and at 60 °C (*on the left*). The spectra are shown in Nyquist (**a**) and Bode (**b**) plots. Full lines represent data calculated from the theoretical model [1]. Potential: 600 mV; electrolyte composition: *filled circle* NaOH, *empty circle* Na^+:K^+ = 3:1, *diamond* Na^+:K^+ = 1:1, *empty square* Na^+:K^+ = 1:3, *filled square* KOH

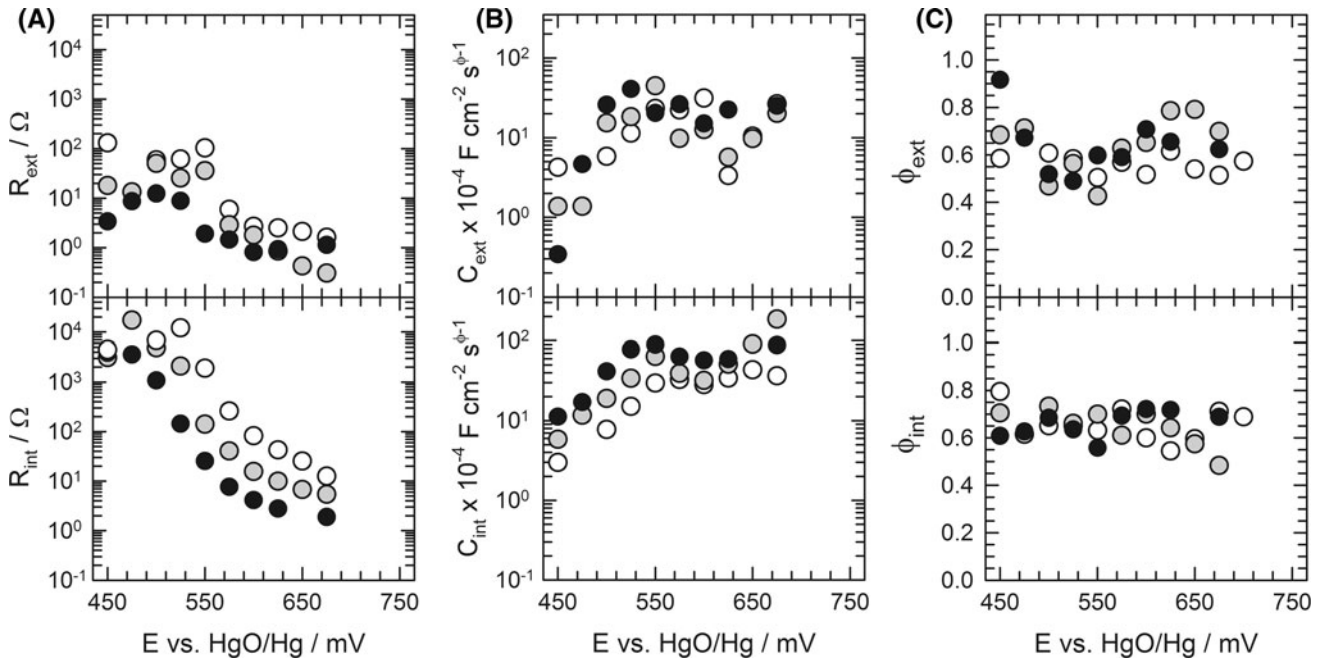

Fig. 5 The fitted values of the equivalent circuit elements: resistance (**a**), capacitance (**b**), and parameter ϕ (**c**) obtained for the individual sublayers in dependence on the anodic polarization potential of the WCI electrode in 14 M NaOH electrolyte at various temperatures: 20 °C *white*, 40 °C *gray*, and 60 °C *black symbols*

relatively high capacitance value of a particular sublayer leading to rapid changes in the system.

3.3 Batch electrolyses

As in the previous cases, the current efficiency of the batch electrolyses was calculated with respect to the ferrate concentration in the anolyte resulting from 3 h electrolysis (Fig. 7). At 20 °C, the highest current efficiency of about 55 % was achieved with NaOH as the electrolyte. The mixed electrolytes demonstrated lower current efficiency (by 10–15 %) than pure KOH, except for the electrolyte containing ions in a ratio of K^+:Na^+ = 3:1 which provided identical results to those of pure KOH. With a temperature increase, the current efficiency gradually decreased in NaOH, while it remained similar for the remaining electrolyte compositions, with the exception of the electrolyte containing ions in a ratio of K^+:Na^+ = 1:1. At 40 °C, maximum efficiency values of around 24 % were achieved with a solution of K^+:Na^+ = 3:1 and in pure KOH, but the efficiency values were well comparable in all solutions used, with the exception of the solution containing ions in a ratio of K^+:Na^+ = 1:3. Here the efficiency retained a value similar to that obtained at a temperature of 20 °C. At 60 °C the trend is clear: the lowest current efficiency of 6 % was observed for pure NaOH. With increasing K^+ content in the solution, the efficiency rapidly increased, reaching a maximum value of 60 % for pure KOH. It is also noteworthy that, after achieving a maximum value relatively rapidly at lower temperatures, the current efficiency again decreases with increasing current density, whereas at 60 °C for pure KOH and electrolytes with high K^+ content the current efficiency remains almost constant (approx. 50 %) for an anode current density up to 20 mA cm^{-2}. This is a positive aspect with respect to the design of a process with high production intensity.

Important complementary information, summarized in Fig. 8, is provided by the concentration of iron in an oxidation state lower than VI+, determined in the anolyte after termination of the synthesis. It permits an explanation of the observed dependences. In agreement with expectations, iron in lower oxidation states displays the highest concentration at 20 °C in pure NaOH. Under these conditions, the iron carbide Fe_3C present in the anode structure dissolves in the anolyte, allowing continuous ferrate synthesis at relatively high current density without any significant inhibition of the electrode surface. This corresponds to the high efficiency of ferrate formation obtained under these operational conditions. The remaining electrolyte compositions were not competitive with this one, most probably due to the low solubility of the dissolution products. At the highest temperature studied, i.e., 60 °C, the situation is different. The low current efficiency observed for pure NaOH solution could be explained by the rapid decomposition of the product at an elevated temperature. However, the iron concentration in lower oxidation states, shown in Fig. 8, does not support this theory. It reaches about half of the value observed at 20 °C. This indicates that the main reason

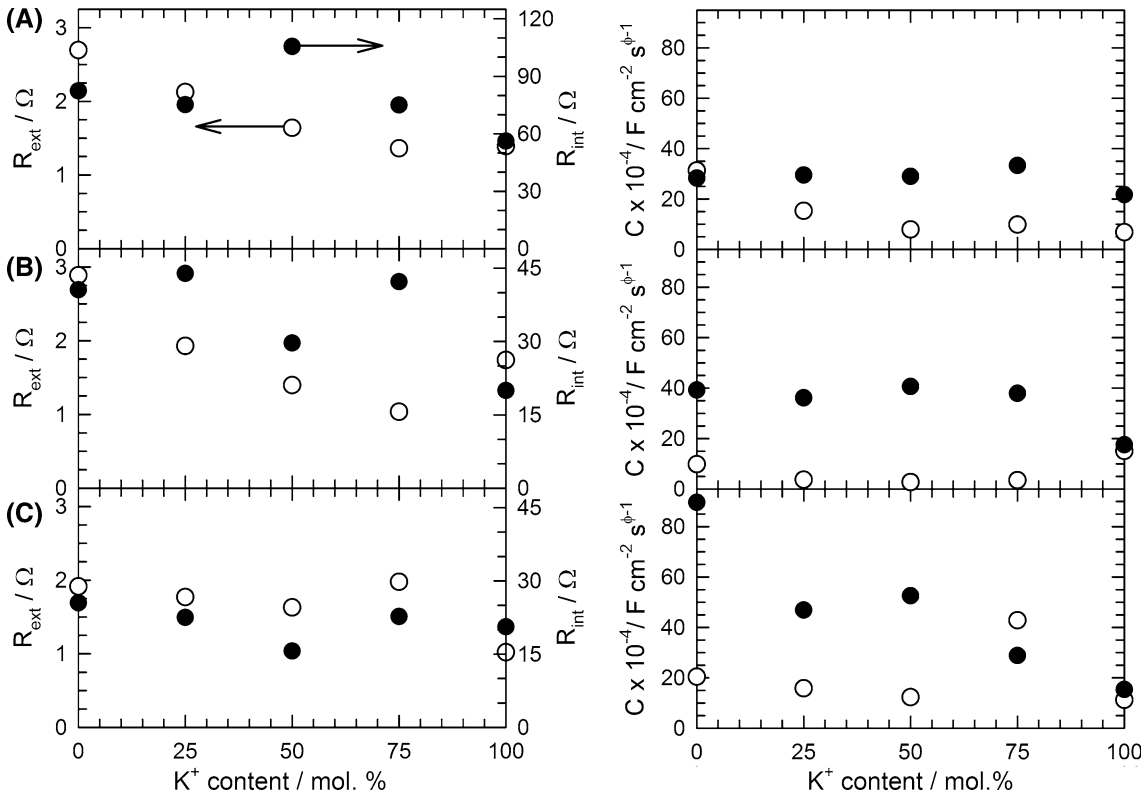

Fig. 6 The fitted values of resistance (*left*) and capacitance (*right*) values obtained for the outer (*empty circle*) and inner (*filled circle*) layers at a potential of 600 mV at 20 °C (**a**), 575 mV at 40 °C (**b**), and 550 mV at 60 °C. (**c**) in dependence on electrolyte composition, i.e., K^+ ion content in the 14 M OH^- solution

for the change in efficiency is the change in the electrode reaction kinetics, especially the relationship between the anodic iron dissolution and oxygen evolution. This is confirmed by the rapid decrease in the resistance of the internal layer with temperature, documented by Fig. 5. In pure KOH solution, the concentration of iron in lower oxidation states remains comparably as low as at 20 °C due to the low solubility of the iron compounds in this environment. Similar to pure iron and SRS, however, at elevated temperatures the efficiency of ferrate production in the solution rich in K^+ ions becomes relatively high. This is especially apparent in the present case of the WCI anode, where the highest efficiency under the conditions studied was obtained at 60 °C in KOH solution. There are two reasons for this behavior, both of which are connected with the structure of the WCI material. The first is the continuous renewal of the anode surface due to the dissolution of the iron carbide phase, which results in the regular removal of the precipitated layer from the anode surface. Only at 60 °C does this process become sufficiently efficient to avoid surface blockage; otherwise the dissolution mechanism changes with the temperature. This circumvents problems lead to the low process efficiency characteristic of the lower temperatures. The second reason is the change in the electrode reaction kinetics with increasing temperature. While in NaOH solution oxygen evolution becomes predominant, in KOH solution iron dissolution remains the predominant reaction. However, an uninhibited anode surface remains a prerequisite for successful ferrate synthesis in this case, too.

The behavior observed at a temperature of 40 °C represents a transition situation. This temperature is already too high for the NaOH electrolyte, but not yet high enough for the solutions rich in K^+ ions. Therefore, the synthesis efficiency observed is comparatively low for all electrolytes and current densities under study.

On the basis of the batch electrolysis results, for the WCI anode the most efficient process conditions were determined to be KOH solution at 60 °C and a current density of approximately 5–15 mA cm^{-2}.

3.4 Metallography and SEM analysis

A metallographic image of the WCI material is shown in Fig. 9. The material is constituted of dark grains of perlite formed by the lamellae of ferrite and cementite (Fe_3C) and cementite phase.

The SEM images of the WCI anode surface taken after 15 min of polarization at 20 °C and 15 mA cm^{-2} are given in Fig. 10. In NaOH, cementite preferentially dissolves from the WCI structure. By contrast, in KOH, cementite

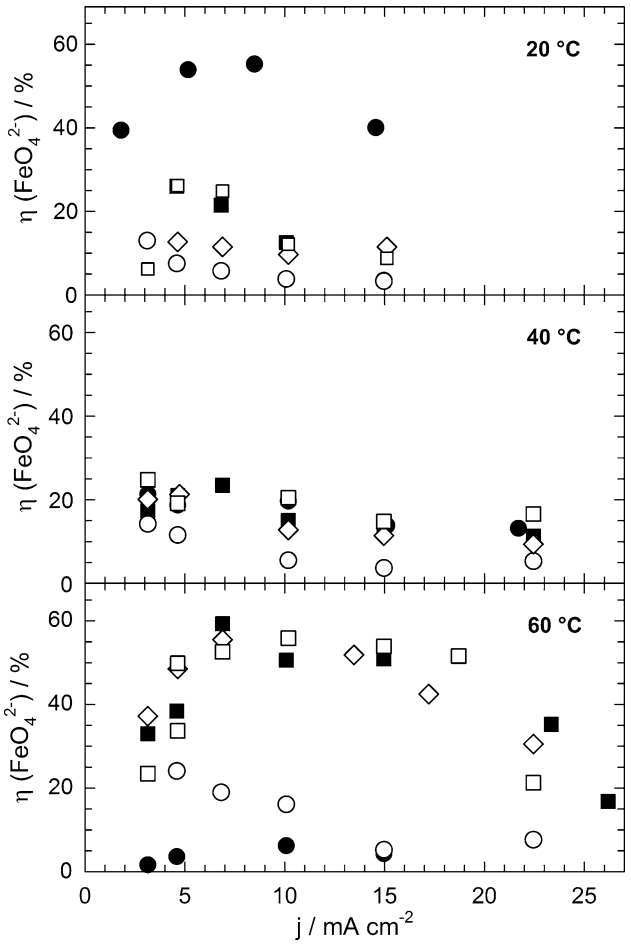

Fig. 7 Dependence of current efficiency of ferrate formation after 180 min of batch electrolysis on anodic current density at various temperatures obtained for the individual electrolytes used: *filled circle* NaOH, *filled square* KOH, *empty circle* Na^+:K^+ = 3:1, *diamond* Na^+:K^+ = 1:1, *empty square* Na^+:K^+ = 1:3; electrode: WCI

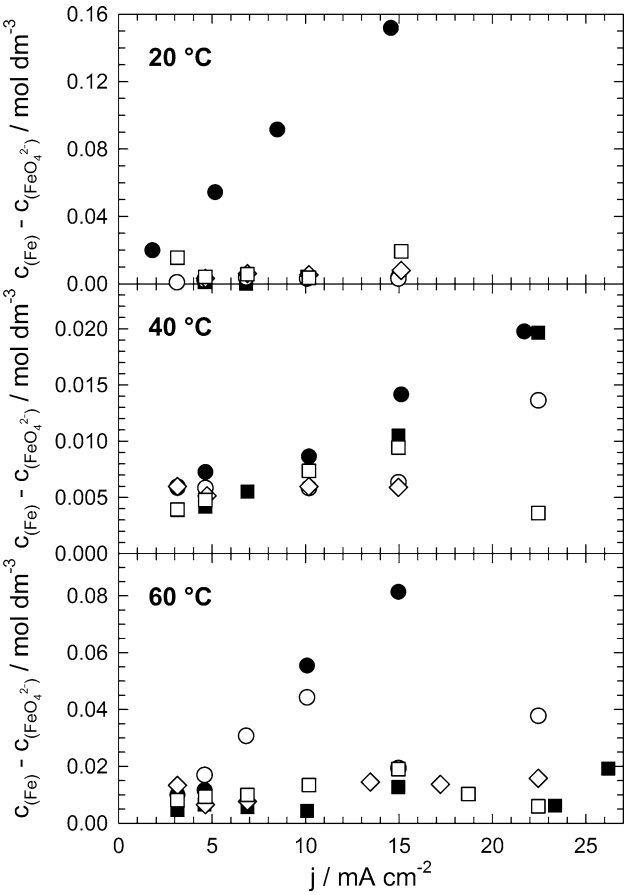

Fig. 8 Dependence of the difference in molar concentration of the total iron and FeO_4^{2-} contained in the anolyte on completion of electrolysis on the anodic current density applied at various temperatures for the individual electrolytes under study: *filled circle* NaOH, *filled square* KOH, *empty circle* Na^+:K^+ = 3:1, *diamond* Na^+:K^+ = 1:1, *empty square* Na^+:K^+ = 1:3; electrode: WCI

dissolves not only from its grains, but also from the perlitic phase where it is present in the form of lamellae.

Similar to the SRS anode, the preferred dissolution of some of the constituents of the anode material structure supports ferrate production. The SEM analysis shown indicates a significant difference in the interaction between the electrolyte and the electrode in the case of NaOH and KOH. KOH provides more intensive dissolution of the iron carbide phase, which is not just limited to the cementite phase as it is in the case of NaOH. Thus, it has the potential to provide electrodes with a higher specific surface and, to a significant degree, with a different surface composition of the anode. It then has an impact on the kinetics of the electrode reaction.

The structure of the anode surface obtained at a temperature of 60 °C is shown in Fig. 11. Similar to the SRS [2], here the electrode surface is covered by a relatively thick hydrated oxide layer, indicating intensive dissolution of the material in both the electrolytes. A detailed analysis

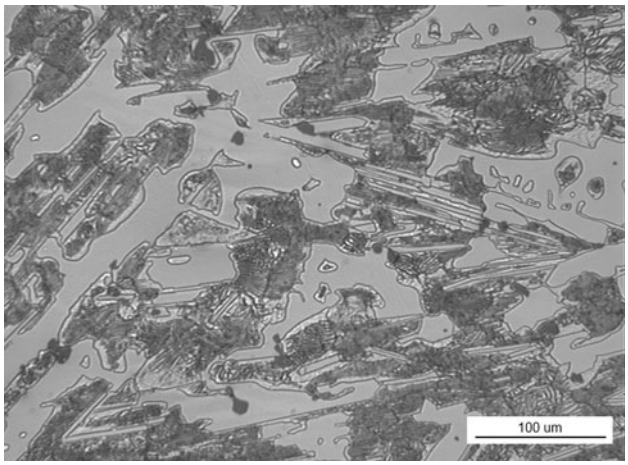

Fig. 9 Metallography of WCI after etching in 2 % nital for 5 min

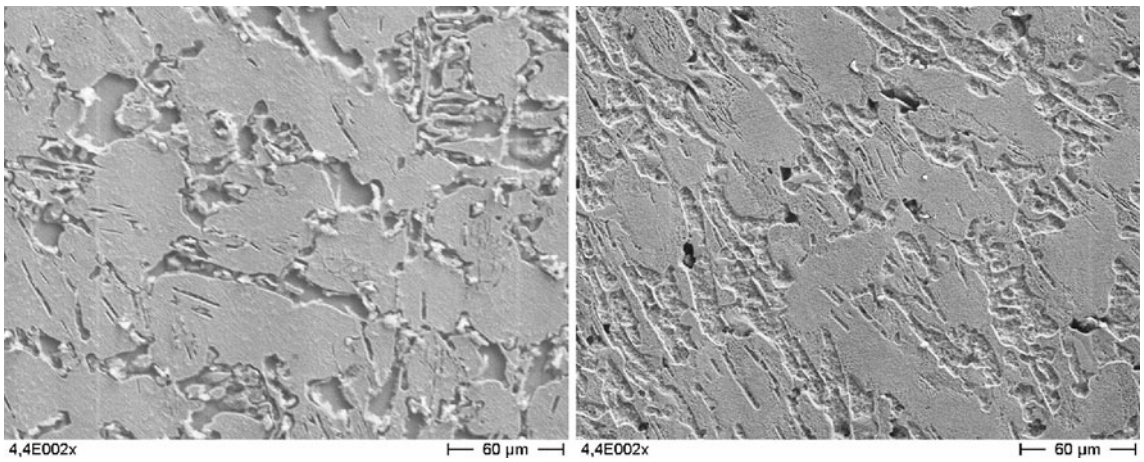

Fig. 10 SEM images of WCI after 15 min anodic polarization at 20 mA cm^{-2} in NaOH (*on the left*) and KOH (*on the right*), temperature 20 °C

of the selectivity of the dissolution of the anode structure is complicated by the fact that the bare surface of the material is not visible. It can be assumed that the mode of dissolution is similar to that at 20 °C. In the case of dissolution in NaOH solution, no evident irregularities in the dissolution of the anode surface can be observed in the photograph. In the electrolytes containing K^+, the surface irregularities are more apparent, which suggests that the anode dissolution is not proceeding homogeneously. Some parts of the structure are preferably dissolved. Based on previous experience, iron carbide is the most probable option. Such intensive dissolution corresponds to the high efficiency of the ferrate production process observed for the WCI anode in KOH solution at 60 °C.

4 Comparison of the individual materials

The aim of this chapter is to summarize the results obtained for the individual materials studied in this series of papers, i.e., pure iron [1], SRS [2] and, in the present manuscript, WCI. This should provide deeper insight into the phenomena observed.

Polarization curves of the individual materials are qualitatively identical. They generally show the same number of current peaks. The current densities of the individual peaks and also, to a certain degree, their potential reflect the protective properties of the passivating layer covering its surface. This is significantly determined by the internal structure of the material. WCI together with SRS generally showed higher current densities, compared to the pure iron electrode. This is especially apparent with increasing temperature and it concerns not only the potential region of current peak AIV, but also regions of active dissolution and passivity. Additionally, peak AIV starts to rise at less anodic potentials. It is also interesting to note the increasing hysteresis of the polarization curve during the reverse potential scan, indicating a significant depassivation of the electrode surface in the transpassive potential region in the case of both the alloyed materials unlike the pure iron electrode. The WCI electrode is further characterized by a strong increase in current peak AII, corresponding to the active dissolution of the material. On the other hand, in the case of SRS in NaOH, a significant increase in the potential region of the material passivity already occurs at 40 °C.

With all materials, the addition of K^+ ion to the electrolyte resulted in a shift of the transpassive region as well as the CIII current peak to less anodic potentials. While with pure iron and SRS, the current density in the passive and the transpassive region decreased, with WCI the trend was the reverse. It is difficult to analyze the reasons for such behavior because both the SRS and the WCI electrodes are characterized by the fairly complex structure of the material. However, the main reason may be seen in the different interaction of Si and iron carbide Fe_3C with the K^+ ion in the electrolyte, which is supported by observations made using SEM. In the case of both alloyed materials (SRS and WCI) the material dissolution rate is enhanced by the preferential dissolution of Si phase in the case of SRS, and cementite, *i.e.*, iron carbide Fe_3C, in the case of WCI. This becomes even more pronounced with increasing temperature.

With EIS, the qualitative behavior of all three materials is similar. They exhibit two time constants, i.e., two semicircles in the Nyquist plot of the spectra, corresponding to the dual structure of the surface oxo-hydroxide films. However, they differ in their detailed characteristics. Firstly, due to its homogeneous structure, the pure iron electrode generally exhibits the highest resistance to dissolution of the materials studied. This corresponds well with the above results. The main difference between all the

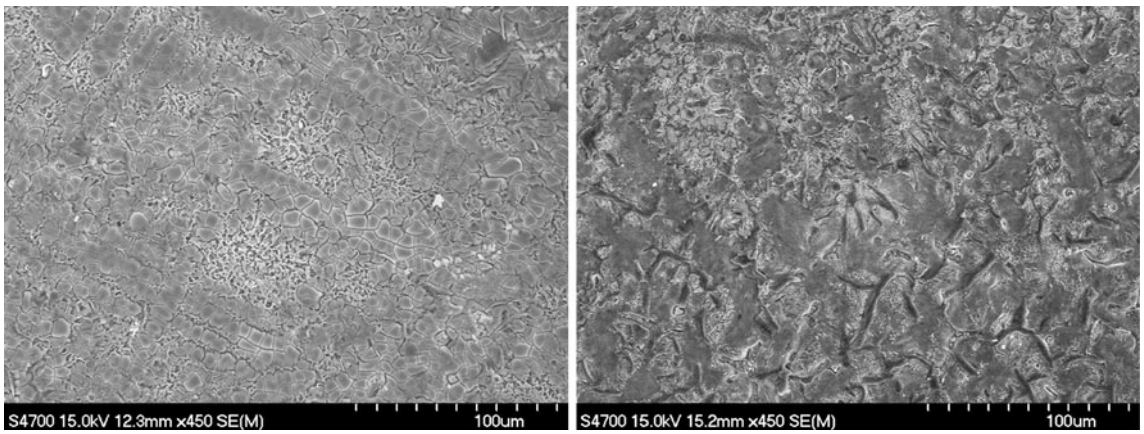

Fig. 11 SEM images of WCI after 15 min anodic polarization at 20 mA cm^{-2} in NaOH (*on the left*) and KOH (*on the right*), temperature 60 °C

materials concerns the properties of the external layer, which are related to the different structure of the materials. With SRS and WCI, the external layer looses its protective properties at a lower temperature and less anodic potentials than pure iron. In the case of the internal protective layer the situation is more interesting. We shall focus mainly on the optimized value of parameter ϕ of the related constant phase element in the equivalent circuit. While in the case of pure iron the value of this parameter increases with the increasing electrode potential from 0.8 to 1.0, in the case of SRS and WCI it decreases in the same potential region from 1.0 to 0.8 or from 0.8 to 0.5, respectively. This indicates that, even under transpassive conditions, the pure iron electrode is covered by a compact surface layer providing at least basic protective properties. With the other two materials it becomes porous and disrupted. In the case of pure iron, the complete destruction of the internal passivating film is first indicated by the EIS data at a temperature of 60 °C and a sufficient anodic potential. For SRS, a temperature of 60 °C is needed to destroy this layer. In the case of WCI, the internal passive layer may be removed at any of the temperatures under study if the electrode potential is sufficiently anodic.

The addition of K^+ ion results in a decrease in the resistance of the surface film. This is related to more progressive interaction between the electrolyte and the surface layer, which negatively influences its compactness. This is especially evident in the case of SRS.

The batch electrolysis results showed that the main difference between pure iron and the remaining two materials exists in their ability to achieve high current efficiency of ferrate synthesis even at enhanced current density. Whereas, with the pure iron anode an increase in the current density typically leads to rapid inactivation of the surface and a decline in ferrate production, in the case of SRS and WCI this phenomenon is significantly less progressive. This confirms the depassivating role of Si as well as Fe_3C. The difference lies in the conditions ensuring the highest current efficiency.

5 Conclusion

A detailed comparative study was performed, targeted to characterize in detail the influence of the anode and anolyte composition on the process of electrochemical ferrate synthesis by iron anode dissolution and oxidation. Representatives of three typical anode materials were used for this purpose: pure iron, SRS, and WCI. The results obtained confirmed the previously proposed theory of the influence of the addition of the main alloying elements on the structure of the two latter materials, i.e., Si and carbon in the form of iron carbide Fe_3C, as a depassivating phase allowing the continuous dissolution of the anode base material. A more detailed investigation of the anolyte composition revealed that this influence is unequally important for these two materials under the individual experimental conditions under study. Generally, the highest current efficiency of ferrate production was obtained for the WCI anode in pure KOH electrolyte at 60 °C. Relatively comparable results were obtained at 20 °C for both SRS and WCI in NaOH solution, although the current efficiency declines more progressively with increasing current density. An alternative worth considering is SRS in KOH at 60 °C. Under these conditions, the current efficiency is lower, but above a current density of 20 mA cm^{-2}, it comes close to WCI in the same environment. Moreover, process efficiency is not as sensitive to the anolyte composition, and the product suspension may be more suitable for its separation. Therefore, it has to be borne in mind as an alternative when electrochemical ferrate production is considered.

The above results are in agreement with the outcomes of voltammetric and EIS data as well as with the SEM analysis of the surface of the anode material after exposure

to the ferrate synthesis environment. The salient information derived from the EIS is that, by predicting the suitability of the anode material for ferrate production, the resistance of the internal protective layer is not the only factor to be considered. Such an approach may incur misleading results since the method does not distinguish between the desired anodic reaction and parasitic oxygen evolution. To distinguish between these two reactions not only the resistance, but also the layer capacity and the ϕ value have to be taken into consideration.

Acknowledgments The authors gratefully acknowledge the financial support for this research by the Ministry of Industry and Trade of the Czech Republic within project No. FR-TI4/363. The authors would also like to express their thanks to Ing. Zuzana Cílová, PhD for the SEM images and the analysis thereof.

References

1. Macova Z, Bouzek K, Sharma VK (2010) J Appl Electrochem 40:1019
2. Macova Z, Bouzek K (2011) J Appl Electrochem 41:1125
3. Bouzek K, Roušar I (1997) J Appl Electrochem 27:679
4. Lescuras-Darrou V, Lapicque F, Valentin G (2002) J Appl Electrochem 32:57
5. Lapicque F, Valentin G (2002) Electrochem Commun 4:764
6. He W, Wang J, Shao H et al (2005) Electrochem Commun 7:607
7. Bouzek K, Roušar I, Taylor MA (1996) J Appl Electrochem 26:925
8. Macova Z, Bouzek K, Hives J et al (2009) Electrochim Acta 54:2673
9. Beck F, Kaus R, Oberst M (1985) Electrochim Acta 30:173
10. Bouzek K, Roušar I, Bergmann H et al (1997) J Electroanal Chem 425:125
11. Zou J-Y, Chin D-T (1988) Electrochim Acta 33:477
12. Híveš J, Mácová Z, Benová M et al (2008) J Electrochem Soc 155:E113
13. Bouzek K, Bergmann H (1999) Corros Sci 41:2113
14. Jüttner K (1990) Electrochim Acta 35:1501